Respected Sir,

Thanks for providing valuable review comments. Please find herewith corrections and justification against review comments for the paper titled “ANN based Over-modulated Space Vector Pulse Width Modulator For VCIM Drives”. You are kindly requested to recommend the paper for journal publication.

Comment-(1): “to reconsider the claim of lower current distortion as it is not apparent from the figures unless the TDH is given”.

Justification/Correction: Table-I is added in the paper which shows the comparison of TDH in phase voltage and phase current for conventional method and proposed overmodulation method.

Comment-(2): “it seems to us that the main merit of the paper is its apriori-given ANN weighting factors, thus reducing the on line computing effort “.

Justification/Correction: Reducing the on line computing effort is in fact is one of the merits of the method, but by Synthesizing and Designing the reference voltage $\overline{V_{sref}}$ (refer equation (19) and (20)) with less harmful harmonics content may further reduces the TDH in the current and voltage which will further reduces the losses. This will makes more suitable to use the method in overmodulation mode-I and mode-II operation. (The above justification is already claimed in conclusion section)

Comment-(3): “the motor plus converter losses comparisons, in overmodulation mode, with the proposed and conventional PWM are needed”.

Justification/Correction: As it is seen from the Table-I, that the proposed method is having less TDH compare to the conventional method. The harmonic current in proposed method is less than the conventional method which will reduce harmonic torque and other losses in drive. Switching frequency is selected such that it should produce minimal switching loss and harmonics loss.

Dr. Rajesh Kumar

ANN BASED OVER-MODULATED SPACE VECTOR PULSE WIDTH MODULATOR FOR VCIM DRIVES

[1]Rajesh Kumar, [2]R. A. Gupta, [3]Rajesh S. Surjuse
[1]Reader, Department of Electrical Engineering, MNIT, Jaipur, India-302017
[2] Prof., Department of Electrical Engineering, MNIT, Jaipur, India -302017
[3] Research Scholar, Department of Electrical Engineering, MNIT, Jaipur, India -302017
rkumar_mnit@rediffmail.com, sujusemnit@rediffmail.com

Abstract: *A high performance overmodulation strategy for PWM voltage-source inverter (VSI) fed induction motor drive is proposed in this paper. Kohonen's Competitive Net based space vector PWM is used to extend its operation from under-modulation (linear mode) to over-modulation (non-linear mode) that is smoothly up to six-step mode. This ANN-based modulator was then incorporated in induction motor drive with rotor flux oriented vector control. This scheme is evaluated under simulation for a variety of operating conditions of the drive. As the full inverter voltage utilization is important from cost and power density improvement perspective, the scheme presents the robust and best strategy for drives operation extended up to six-step mode.*

Key words: *Space Vector Pulse Width Modulation (SVPWM), Modulation Index, Vector Controlled Induction Motor (VCIM), Kohonen's Competitive Net.*

1. Introduction

The carrier-based pulse width modulation (PWM) methods are the preferred approach in most drive applications due to the low harmonic spectrum, the fixed switching frequency and the implementation simplicity. Carrier-based PWM operation can be divided into two modes [1] :

- Linear Mode: In this mode of operation, the peak of a modulation signal is less than or equal to the peak of the carrier signal. When the carrier frequency is greater than twenty times modulation signal frequency, the gain of PWM is nearly equal to 1 ($G \approx 1$).
- Nonlinear Mode: In this mode of operation, the peak of a modulation signal is greater than the peak of the carrier signal, over-modulation occurs with $G<1$. The six-step mode makes the end of the nonlinear mode.

Carrier-based PWM is further classified [2] into suboscillation method and space vector pulse width modulation (SVPWM). In suboscillation method the maximum value of the modulation index (m) is 0.785 reached at a point where the amplitudes of the reference and the carrier signal become equal. In SVPWM the maximum modulation index extends up to 0.907.

Drive operation in the nonlinear modulation range i.e. in over-modulation range had following problems [3]: 1) large amounts of sub-carrier frequency harmonic currents are generated; 2) the fundamental component voltage gain significantly decreases and 3) the switching device gate pulses are abruptly dropped.

In current-controlled drives [4]-[7], overmodulation operation results into sub-carrier frequency harmonic distortion and current regulator performance reduction,. The current regulators are heavily burdened by the feedback current sub-carrier frequency harmonics, regulator saturation and oscillatory operations. On the other hand, full inverter voltage utilization is important from cost and power density improvement perspective. Also a drive with high performance over-modulation range operating capability is less sensitive to inverter dc-bus voltage sag and hence increases drive reliability. Recently over-modulation issues have attracted the attention of many researchers. Neural network based over-modulation implementation has many advantages such as gives higher switching frequency, lesser harmonics and robust control [8]-[12]. Section–II presents the behavior of field oriented control under overmodulation. Section-III and IV present conventional and neural network based SVPWM in voltage source inverter respectively. The proposed ANN-based overmodulation strategy is presented in section–V, for the SVPWM voltage-source inverter and was incorporated in rotor flux oriented vector control induction motor drive.

2. Field Oriented Control

The field oriented induction machine model, shows the decoupled system that results when current coincidence exists (necessary condition) and the slip is selected to maintain the q-axis rotor flux at zero (sufficient condition). To achieve current coincidence, a current regulator is often employed. Early attempts at current regulation were simple implementations of a stationary frame PI regulator. The stationary PI is recognized to have nonzero steady state error, but the high gain of the stationary compensator and inverter reduces the phase lag between the command and feedback current while in the linear region.

However, the unique characteristics of the stationary PI make it inherently unsuited for Field oriented control (FOC) regardless of the additional compensation techniques employed [6]. The controller was transformed to the synchronous frame wherein all quantities are dc as in Fig. 1. Independent control of each component of current, flux producing current

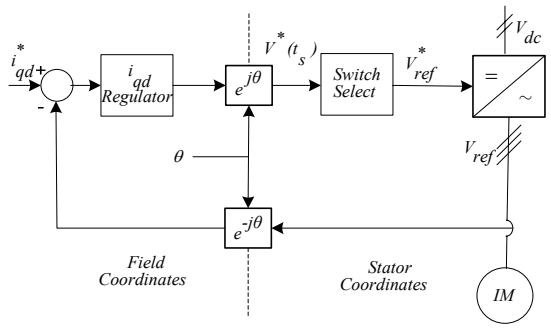

Fig.1. Field coordinate model of the PI current regulator.

i_d and torque producing current i_q is impossible due to the cross coupling that naturally occurs regardless of the compensator gains. Adding command feed forward or state variable feedback lessens the adverse effects of the stationary PI. However, the nonlinear gain of the inverter $(G(V^*))$ counteracts the added compensation and diminishes its benefits.

The nonlinear gain also affects the control by forcing the current regulator to compensate for incorrect voltage vectors applied to the terminals of the machine. Consider the field coordinate current regulator's voltage command after conversion to stator coordinates $V^*(t_s)$. The type of current regulator, whether proportion/integra1, predictive current control, pulse width control, trajectory tracking control [13]-[14], etc., alters the dynamic response of the control, but not the effect of the inverter's characteristics on the drive system.

The command voltage vector, $V^*(t_s)$, is the input to the space vector PWM generator. In the linear region, the output vector, $\overline{V_{ref}}$, has three components V_i, V_{i+1} and V_0. The V_i vector is applied for a duration of T_i; the V_{i+1} vector applied for T_{i+1}; and the zero vector applied for T_0. T_s is the period of the carrier as stated by equation (3) to equation (5). By complying with the law of pulse width modulation, the PWM inverter, on a fundamental component basis, behaves as a linear amplifier with the gain a function of the bus voltage. With the switching frequency finite and the space vector modulator in the linear region, the output voltage is given by

$$\overline{V_{ref}} = G(V_{dc}) * \overline{V^*_{ref}} \qquad (1)$$

The transition region begins when the command vector touches the side of the hexagon; the zero vector's on time is zero $(T_0 = 0)$. This region requires an overmodulation strategy to increase the output voltage. Furthermore, current regulators demand an overmodulation algorithm with good transition region dynamics. For example, the modulator must deliver the voltage command, $\overline{V^*_{ref}}(t)$, which includes steady state and transient voltage components, as commanded by the current loop without saturating the current loop. Fig. 3. shows this voltage vector in the first sector. Space vector PWM, however, delivers a vector that results in a fundamental voltage given by $V_{ref}(t)$. If not corrected by an overmodulation strategy, then the error, $V_e(t)$, must be accumulated within the current regulator. The space vector PWM modulator produces the unintended effect of cross coupling the stator circuits. The inability to apply the correct voltage vector-phase and magnitude to ensure current coincidence degrades the quality of the FOC; in the extreme case, it invalidates the necessary and sufficient conditions for field orientation.

The objective of overmodulation algorithm is to compensate the modulating wave in phase and magnitude to account for bus variation and the reduced gain while maintaining a unity transfer function. The scheme for vector control induction motor drive with neural network based space vector modulated VSI is shown in Fig. 2.

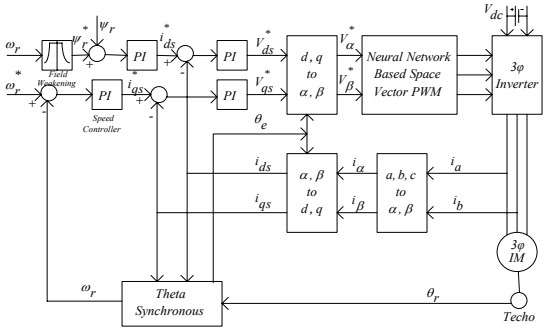

Fig. 2. Vector control Induction Motor Drive with neural network based space vector modulated VSI.

3. Conventional SVPWM in voltage source inverter

In voltage source inverter [1]-[3], depending on the switching states, the space vector of the stator phase voltages can be in six different positions and there are two zero vectors, corresponding to the cases when the three inverter terminals are connected either to the positive or to the negative rail of the d.c. supply. The six non-zero voltage space vectors form a hexagonal locus. The zero space vectors are located at the origin of the reference frame. Any desired stator voltage space vector inside the hexagon can be obtained from the weighted combination of the eight switching vectors. It is the goal of the space vector modulation technique to reproduce the reference stator voltage space vector by using the appropriate switching vector, under the constrain of minimal harmonic current distortion and with shortest possible cycle time.

In order to reduce the number of switching actions and to make full use of active turn on time for space vectors, the vector $\overline{V_{sref}}$ is split into the two nearest

adjacent voltage vectors and zero vectors $\overline{V_0}$ and $\overline{V_7}$ in an arbitrary sector. For Sector 1 in one sampling interval, vector $\overline{V_{sref}}$ can be given as

$$\overline{V_{sref}} = \frac{T_1}{T_s}\overline{V_1} + \frac{T_3}{T_s}\overline{V_3} + \frac{T_7}{T_s}\overline{V_7} + \frac{T_0}{T_s}\overline{V_0} \quad (2)$$

where $T_s - T_1 - T_3 = T_0 + T_7 \geq 0$, $T_0 \geq 0$ and $T_7 \geq 0$

The length and angle of $\overline{V_{sref}}$ are determined by vectors $\overline{V_1}, \overline{V_2}, \ldots\ldots \overline{V_6}$ that are called active vectors and $\overline{V_0}$, $\overline{V_7}$ are called zero vectors. In general

$$\overline{V_{sref}}T_s = \overline{V_i}T_i + \overline{V_{i+1}}T_{i+1} + \overline{V_7}T_7 + \overline{V_0}T_0 \quad (3)$$

where T_i, T_{i+1}, T_7, T_0 are respective on duration of the adjacent switching state vectors $(\overline{V_i}, \overline{V_{i+1}}, \overline{V_7} and \overline{V_0})$. The on durations are defined as follows:

$$T_i = mT_s Sin(60-\theta) \quad (4)$$

$$T_{i+1} = mT_s Sin(\theta) \quad (5)$$

$$T_7 + T_0 = T_s - T_i - T_{i+1} \quad (6)$$

Where *m* is modulation index defined as :

$$m = \frac{2}{\sqrt{3}}\frac{\left|\overline{V_{sref}}\right|}{V_{dc}} \quad (7)$$

V_{dc} is d.c. bus voltage and θ is angle between the reference vector $\overline{V_{sref}}$ and the closest clockwise state vector as depicted in Fig. 3.

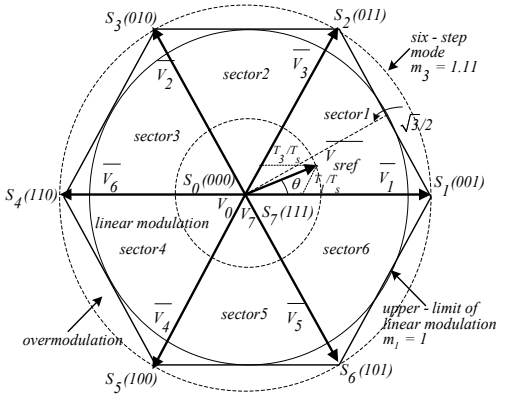

Fig. 3. Linear and overmodulation ranges in SVPWM.

4. Neural Network Based SVPWM In VSI

In a voltage source inverter the space vector modulation technique requires the use of the adjacent switching vectors to the reference voltage vector and the pulse times of these vectors. For this purpose, the sector where the reference voltage vector is positioned must be determined. This sector number is then used to calculate the position θ of the reference voltage vector with respect to the closest clockwise switching vector (Fig. 3). The pulse time can than be determined by using the trigonometric function $Sin(\theta)$ and $Sin(60-\theta)$ as in equation (4) and equation (5).

However, it is also possible to determine the two non-zero switching vectors which are adjacent to the reference voltage vector by computing the cosine of angles between the reference voltage vector and six switching vector and then by finding those two angles whose cosine values are the largest. Mathematically this can be obtained by computing the real parts of the products of the reference voltage space vector and the six non-zero switching vectors and selecting the two largest values [9] and [12]. These are proportional to $Cos(\theta)$ and $Cos(60-\theta)$ respectively. Where θ and $(60-\theta)$ are the angles between the reference voltage vector and the adjacent switching vectors.

It is also possible to use an ANN based on Kohonen's competitive layers. In this paper modified Kohonen's competitive layers is proposed. It has two winner neurons and the outputs of the winner neurons are set to their net inputs. If normalized values of the input vectors are used, then the six outputs (six net values $n_1, n_2, \ldots\ldots n_6$) will be proportional to the *cosine* of the angle between the reference voltage vector and one of the six switching vectors. The two largest net values are then selected. These are n_i and n_{i+1}, proportional to $Cos(\theta)$ and $Cos(60-\theta)$. Since the space vector modulation is a deterministic problem and all classes are known in advance, there is no need to train the competitive layer.

$$net = V_{sref}.W = \left|V_{sref}\right||W|Cos(\theta) \quad (8)$$

Since the input vector and the weight vector are normalized, the instars net input gives the *cosine* of the angles between the input vector and the weight vectors that represent the classes. The largest instar net input wins the competition and the input vector is then classified in that class. The winner of the competition is the closest vector to the reference vector.

The six net values can be written in a matrix form for all neurons as:

$$\begin{bmatrix} n_1 \\ n_2 \\ n_3 \\ n_4 \\ n_5 \\ n_6 \end{bmatrix} = \begin{bmatrix} 1 & -1/2 & -1/2 \\ 1/2 & 1/2 & -1 \\ -1/2 & 1 & -1/2 \\ -1 & 1/2 & 1/2 \\ -1/2 & -1/2 & 1 \\ 1/2 & -1 & 1/2 \end{bmatrix} \begin{bmatrix} V_{Aref} \\ V_{Bref} \\ V_{Cref} \end{bmatrix} \quad (9)$$

where

$$\overline{W} = \begin{bmatrix} 1 & 1/2 & -1/2 & -1 & -1/2 & 1/2 \\ -1/2 & 1/2 & 1 & 1/2 & -1/2 & -1 \\ -1/2 & -1 & -1/2 & 1/2 & 1 & 1/2 \end{bmatrix}^T , \overline{V_{sref}} = \begin{bmatrix} V_{Aref} \\ V_{Bref} \\ V_{Cref} \end{bmatrix}$$

Assuming V_{sref} is applied to the competitive layer and n_i and n_{i+1} are the neurons who win the competition. Then from equation (8) we have

$$\begin{bmatrix} n_i \\ n_{i+1} \end{bmatrix} = \left|\overline{V_{sref}}\right| \begin{bmatrix} Cos(\theta) \\ Cos(60 - \theta) \end{bmatrix} \quad (10)$$

Also

$$\begin{bmatrix} Cos(\theta) \\ Cos(60 - \theta) \end{bmatrix} = \frac{2}{\sqrt{3}} \begin{bmatrix} 1/2 & 1 \\ 1 & 1/2 \end{bmatrix} \begin{bmatrix} Sin(60-\theta) \\ Sin(\theta) \end{bmatrix} \quad (11)$$

Using equation (10) and equation (11) we get

$$\frac{2}{3}\frac{T_s}{V_{dc}} \begin{bmatrix} -1 & 2 \\ 2 & -1 \end{bmatrix} \begin{bmatrix} n_i \\ n_{i+1} \end{bmatrix} = \frac{2}{\sqrt{3}} \frac{\left|\overline{V_{sref}}\right|}{V_{dc}} \begin{bmatrix} Sin(60 - \theta) \\ Sin(\theta) \end{bmatrix} T_s \quad (12)$$

Equation (12) is the on duration of the consecutive adjacent switching state vector V_i and V_{i+1}, which is same as equation (4) and equation (5).Therefore we have

$$\begin{bmatrix} T_i \\ T_{i+1} \end{bmatrix} = \frac{2}{3}\frac{T_s}{V_{dc}} \begin{bmatrix} -1 & 2 \\ 2 & -1 \end{bmatrix} \begin{bmatrix} n_i \\ n_{i+1} \end{bmatrix} \quad (13)$$

The implementation of this method is depicted in Fig. 4., first n_k for $k=1\ldots\ldots6$ are calculated. Two

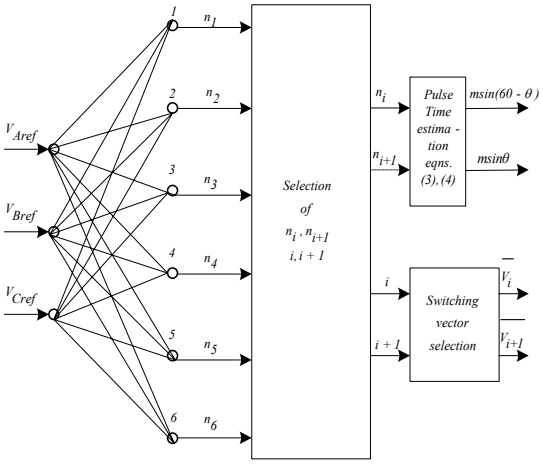

Fig. 4. Modified Kohonen's competitive layer based implementation of the space vector modulation technique for VSI.

largest n_i, n_{i+1} and their corresponding indexes (i.e. i and $i+1$) are selected by Kohonen's competitive network. The on duration (T_i and T_{i+1}) of the two adjacent space vectors are computed. The space vector $\overline{V_i}$ and $\overline{V_{i+1}}$ are selected according to the value of i and $i+1$. When adjacent vectors and on times are determined the procedure for defining the sequence for implementing the chosen combination is identical to that used in conventional space vector modulation.

5. Overmodulation Implementation In SVPWM

As the modulation index increases, the radius of the circular trajectory in the linear region increases until at $m_1 = 1$, it becomes the circle inscribed by the hexagon. For this value of modulation index, the on duration of the zero vector reduces to zero , when the reference vector touches the hexagon at $\theta = (2k + 1)\Pi/6$ where $k = 0,1,---5.$ This is the upper limit of the linear modulation [9]-[12]. Further increase in modulation index while keeping a circular voltage vector to smoothly deviate from a sinusoidal circular trajectory reaching ultimately a discrete six-step switching sequence. For continuous control over the modulation index, the transition from the sinusoidal modulation to six-step operation is divided into two modes, namely mode I and mode II. The maximum output voltage in mode I and mode II are obtained at $m_2 = 1.05$ and $m_3 = 1.1$ respectively. Based on the modulation index, the selector chooses among linear modulation, overmodulation mode I and overmodulation mode II.

A. Overmodulation Mode I

In overmodulation Mode I, the reference vector is distorted at a specific angle and the distorted vector $\overline{V_{sref}}$ is allowed to move along the hexagon side until the requested modulation index is obtained. The on duration of the zero vector is zero, as long as the end of this vector remains on the hexagon side. The maximum attainable modulation index in this mode of operation m_2 is reached when the distorted reference vector remains on the hexagon side for all θ.
Here

$$T_i + T_{i+1} = T_s \quad (14)$$

Putting T_i and T_{i+1} above from (3) and (4) gives

$$m = \frac{1}{\sin\theta + \sin(60-\theta)} \quad (15)$$

For this m, the on durations of the adjacent active switching vector are given by

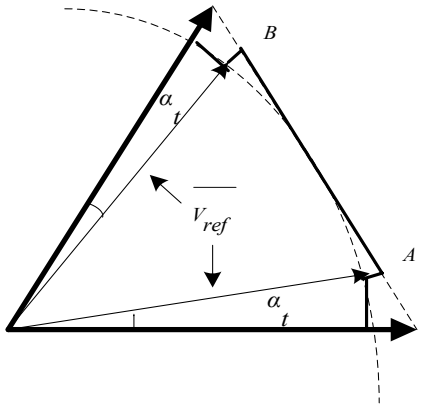

Fig. 5. Reference vector trajectory in overmodulation mode I

$$T_i = \frac{sin(60-\theta)}{sin\theta+sin(60-\theta)} T_s = \frac{msin(60-\theta)}{msin\theta+msin(60-\theta)} T_s \quad (16)$$

$$T_{i+1} = T_s - T_i \quad (17)$$

If α_t is the voltage reference angle at which the transition from circular sinusoidal trajectory to the hexagon takes place, the average modulation index over *AB* in Fig. 5. therefore can be calculated from

$$m = \frac{2}{(\Pi/3-2\alpha_t)} \int_{\alpha_t}^{\Pi/6} \frac{1}{cos(\Pi/6-\alpha)} d\alpha \quad (18)$$

which gives

$$m = \frac{1}{2} \frac{1}{(\Pi/6-\alpha_t)} ln \frac{1+sin(\Pi/6-\alpha_t)}{1-sin(\Pi/6-\alpha_t)} \quad (19)$$

Since at $\theta = 30^0$, $msin\theta$ and $msin(60-\theta)$ are equal, the modulation index can easily be obtained from the addition of these two at $\theta = 30^0$. For all other angles, m remains unchanged. Using this technique, the instantaneous modulation index will be modified six times during one period of the reference voltage. In this mode m as a function of $msin\alpha_t$ is calculated and stored in the form of a lookup table. For a given value of m, the corresponding $msin\alpha_t$ can be reasonably approximated. A decision then is made based upon a comparison between the calculated $msin\alpha_t$ and the $msin\theta$ output of the network of Fig. 2. The on duration of the corresponding switching vectors then are calculated either from (3)-(5), for end of reference vector on circular trajectory or from (16)-(17), for end of reference vector on the hexagon side.

B. Overmodulation Mode II

In overmodulation Mode II, the modulation index further increases from $m_2 = 1.05$ to $m_3 = 1.1$ of the six-step maximum.

The reference voltage vector $\overline{V_{sref}}$ is distorted in both magnitude and phase angle. The trajectory of the distorted reference vector jumps from a discrete six-step switching to a continuous hexagon side at a specific angle (α_h). Such a switching method is identified by a hold angle α_h, which controls the time the distorted reference remains at the vertices. From the fundamental component of the distorted voltage as shown in Fig. 6., the modulation index as a function

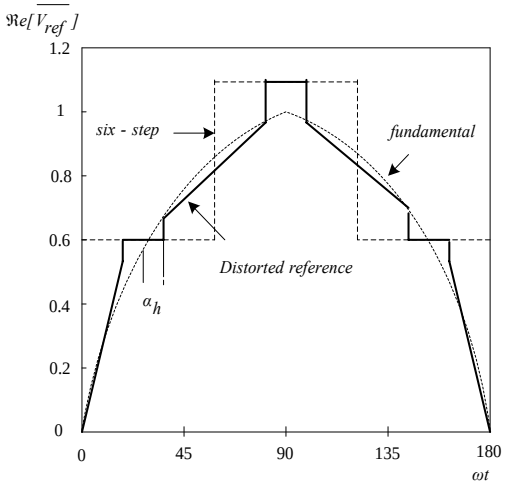

Fig. 6. Distorted reference voltage in overmodulation mode II

of α_h is given by

$$m = \frac{4\sqrt{3}}{\Pi^2}(2\alpha_h cos(\Pi/6 - \alpha_h) + 2sin(\Pi/6 - \alpha_h) + \alpha_h cos(\Pi/6 + \alpha_h) - \alpha_h sin(\Pi/6 + \alpha_h) + \alpha_h sin\alpha_h + cos\alpha_h) \quad (20)$$

In this mode, m as a function of $msin\alpha_h$ is calculated and stored in the form of a lookup table. For a given value of m, the corresponding $msin\alpha_h$ can be reasonably approximated. A decision then can be made based upon a comparison between the calculated and the current $msin\theta$ from the network in Fig. 2. and appropriate switching vectors are switched accordingly. Fig. 7. presents the proposed strategy for continuous operation from linear modulation to overmodulation for SVPWM inverter.

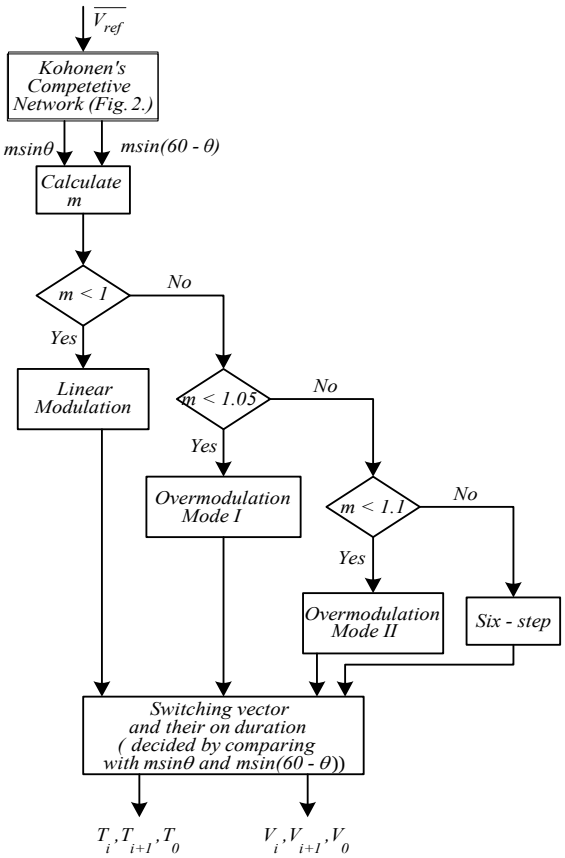

Fig. 7. Linear modulation to overmodulation strategy for SVPWM inverter

from six-step to PWM mode when modulation index decreases form 1.1 to 0.8. Fig. 13. shows time responses of speed, current, torque and duty-cycle for vector control induction motor drive with dynamic

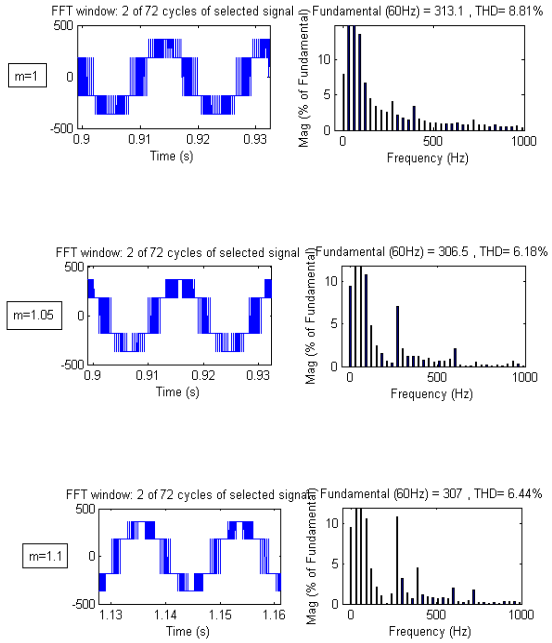

Fig. 8. Phase Voltages and their spectra in the overmodulation region with proposed method for various modulation index.

6. Simulation Results with Overmodulated SVPWM

In SVPWM switching harmonics are suppressed to a large extent by the low-pass characteristic of the machine inductances and by the inertia of the mechanical system. The remaining distortions of the current waveforms and the electromagnetic torque can be valued by performance criteria. Although the torque harmonics are produced by the harmonic currents, there is no stringent relationship between both of them. Lower torque ripple can go along with higher current harmonics and vice versa. The simulation results of ANN-based overmodulation strategy are presented in Fig. 8. to Fig.13. for the SVPWM voltage-source inverter based rotor flux oriented vector control induction motor drive. Fig. 8. and Fig. 9. shows phase voltages and their spectra in the overmodulation region with ANN based proposed method and conventional method respectively. Fig. 10. and Fig.11. shows phase currents and their spectra in the overmodulation region with ANN based proposed method and conventional method respectively. The switching frequency was at 3 kHz and with constant load of 8 Nm. Table-I present the comparison of TDH in both the methods at different modulation index. The data shows less TDH for proposed method and hence less losses. Fig. 12. shows the phase current transition

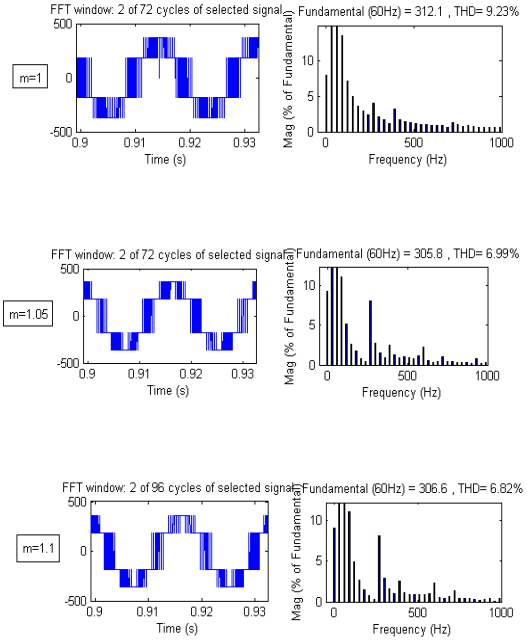

Fig. 9. Phase Voltages and their spectra in the overmodulation region with conventional method for various modulation index.

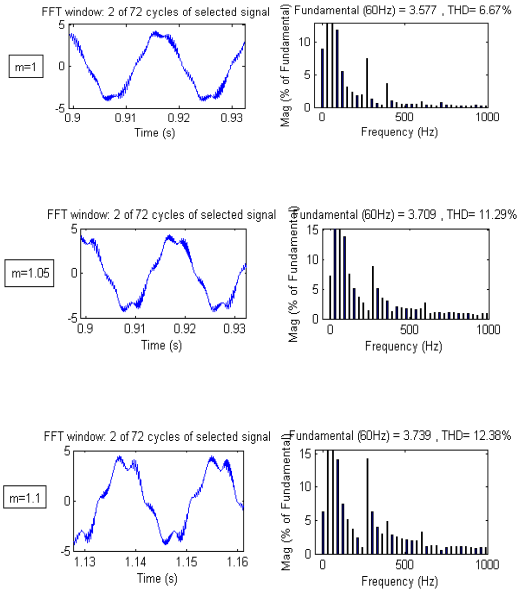

Fig. 10. Phase currents and their spectra in the overmodulation region with proposed scheme for various modulation index.

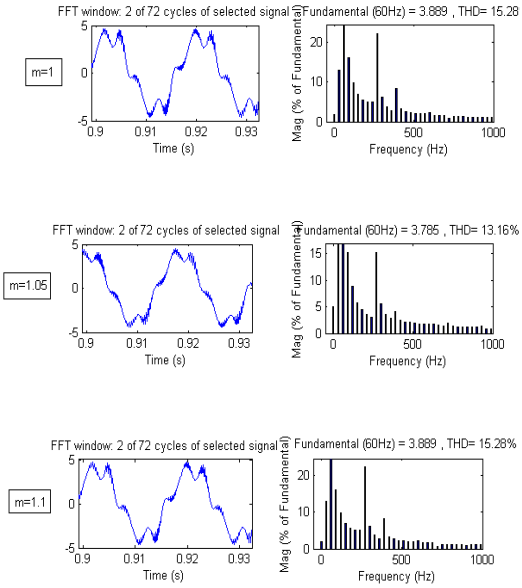

Fig. 11. Phase currents and their spectra in the overmodulation region with conventional method for various modulation index.

overmodulation behavior (for m=1.1) under speed reversal and at constant load torque. The results shows better over all performance of ANN based overmodulation strategy for vector control induction motor drive.

TABLE -I
COMPARISON OF TDH IN CONVENTIONAL METHOD AND PROPOSED OVERMODULATION METHOD

Phase Voltage TDH

Modulation Index (m)	Conventional Method TDH (in % of fundamental)	Overmodulation Method TDH (in % of fundamental)
1	9.23	8.81
1.05	6.99	6.18
1.1	6.82	6.44

Phase current TDH

Modulation Index (m)	Conventional Method TDH (in % of fundamental)	Overmodulation Method TDH (in % of fundamental)
1	15.2	6.67
1.05	13.1	11.29
1.1	15.28	12.38

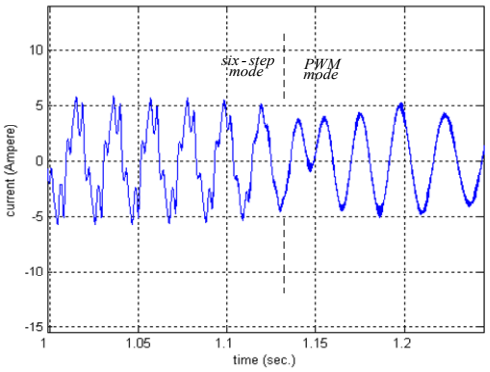

Fig. 12. Transition from six-step to PWM mode.

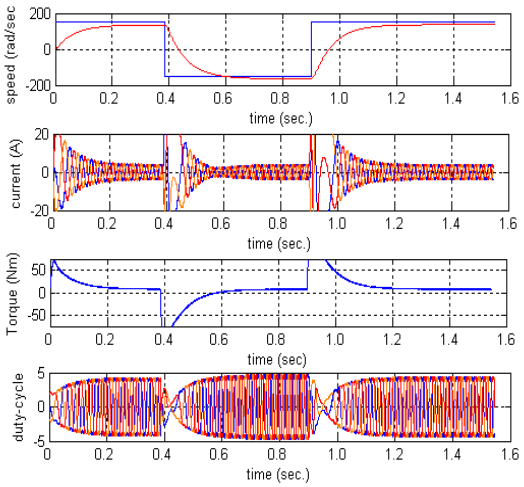

Fig. 13.Vector control induction motor drive with dynamic overmodulation behavior (for m=1.1) under speed reversal and constant load torque.

7. Conclusion

ANN based SVPWM has been described, that operates very well in undermodulation as well as in overmodulation including mode-I and mode-II regions. The scheme is evaluated with rotor flux oriented vector controlled induction motor drive. The ANN based SVPWM can give higher switching frequency, which is not possible with conventional DSP based SVPWM. Also the distortion of the reference vector in the overmodulation region is reduced, resulting in reduced output distortion and less losses in the drive. The drive performance was best under dynamic operation.

Appendix

The parameters of induction motor are as follows:

P	Nominal power	2.2KW
R_s	Stator resistance	1.77 ohms
R_r	Rotor resistance	1.34 ohms
X_{ls}	Stator leakage reactance	5.25 ohms
X_{lr}	Rotor leakage reactance	4.57 ohms
X_m	Mutual reactance	139 ohms
J	Rotor inertia	0.025 Kg.m^2
p	Number of pole	4

References

1. Keliang Zhou and Danwei Wang, "Relationship between space vector modulation and three phase carrier- based PWM: A comprehensive analysis", *IEEE Trans. on Industrial Electronics*, *vol. 49, No.1,* Feb. 2002, pp 186-196.

2. Joachim Holtz, "Pulse width modulation- A survey", *IEEE Trans. on Industrial Electronics*, *vol.39, No.5*, Dec.1992, pp 410-420.

3. Ahmet M. Hava, Russel J. Kerkman and Thomas A. Lipo, " Carrier-based PWM-VSI overmodulation strategies: Analysis, comparison and design", *IEEE Trans. on Power Electronics*, *vol. 13, No.4*, July 1998, pp. 674-688.

4. Ahmet M. Hava, Seung-Ki Sul, Russel J. Kerkman and Thomas A. Lipo, "Dynamic overmodulation characteristics of triangle intersection PWM method," *IEEE Trans. on Industry Applications*, *vol. 35, No.4*, July/August 1999, pp. 896-907.

5. J. Holtz, W. Lotzkat and A. M. Khambadkone, "On continuous control of PWM inverters in the overmodulation range including the six-step mode," *IEEE Trans. on Power Electronics*, *vol. 8, No.4*, October 1993, pp. 546-553.

6. Russel J. Kerkman , D. Leggate, B. J. Seibel and T. M. Rowan, "Operation of PWM voltage source-inverters in the overmodulation region," *IEEE Trans. on Industrial Electronics*, *vol. 43, No.1*, July 1996, pp. 132-141.

7. D. W. Chung, J. S. Kim and S. K. Sul, "Unified voltage modulation technique for real-time three-phase power conversion" *IEEE Trans. on Industry Applications*, *vol. 34, No.2,* March/April1998, pp. 374-380.

8. J. O. P. Pinto, B. K. Bose, L. E. B. da Silva and M. P. Kazmierkowski, "A neural-network-based space-vector PWM controller for voltage fed inverter induction motor drive" *IEEE Trans. on Industry Applications*, *vol. 36, No.6*, Nov./Dec.2000, pp. 1628-1636.

9. A. R. Bakhshai, Geza Joos, P. K. Jain and Hua Jin, " Incorporating the overmodulation rang in space vector pattern generators using a classification algorithm" *IEEE Trans. on Power Electronics*, *vol. 15, No.1,* January 2000, pp. 83-91.

10. C. Wang, B.K. Bose, V. Oleschuk and J.O.P Pinto, "Neural Network based space vector PWM of a three level inverter covering overmodulation region and performance evaluation on induction motor drive" *Proc. Conf. Rec.of IEEE IECON,* 2003, pp. 1-6.

11. N. P. Filho, J. O. P. Pinto, L. E. B. da Silva and B. K. Bose, "A simple and ultra-fast DSP-based space vector PWM algorithm and its implementation on a two-level inverter covering undermodulation and overmodulation" *Proc. Conf. Rec. of IEEE Industrial Electronics, Korea,* Nov.2004, pp. 1224-1229.

12. M. Saeedifard and A. R. Bakhsahai, "Vector classification and voltage control in PWM three-level inverters", *Proc. Conf. Rec. of IEEE Power Electronics, Germany*, 2004, pp. 4411-4417.

13. J. Holtz and N. Oikonomou, "Synchronous optimal pulsewidth modulation and stator flux trajectory control for medium voltage drives", *IEEE Trans. on Industry Applications*, *vol. 43, No.2,* March./April 2007, pp. 600-608.

14. N. Oikonomou and J. Holtz, "Closed-loop control of medium voltage drives operated with synchronous optimal pulsewidth modulation", *IEEE Trans. on Industry Applications*, *vol. 44, No.1*, Jan./Feb. 2008, pp. 115-123.